Universal structural phase transition in network glasses

M. Stevens and P. Boolchand
Physics Department, University of Cincinnati, Cincinnati, Ohio 45221

J. G. Hernandez
Energy Conversion Devices, Troy, Michigan 48084

(Received 29 May 1984)

Raman and Mössbauer spectroscopy provide evidence for a transition from a molecular-cluster network at $x=0$ to a continuous network at $x=0.35$ in $Ge_{1-x}Sn_xSe_2$ alloy glasses. The nature of this morphological transition can be understood in terms of a reformation of molecular-cluster surfaces in the heterogeneous phase to yield a homogeneous phase. The transition is believed to be a universal property of covalent networks and can be effected in one of several ways. In the present experiments, this transition has been stimulated by alloying, i.e., chemical tuning of cation constraints.

I. INTRODUCTION

Until a few years ago it was fashionable to discuss the structure of stoichiometric melt-quenched network glasses in terms of chemically ordered continuous random networks (CRN's).[1] Glasses of the type AB_2, such as SiO_2, GeS_2, and $GeSe_2$, in analogy to a-Ge, for example, were taken to be random networks of geometrically well-defined $A(B_{1/2})_4$ tetrahedral building blocks.

The availability of new spectroscopic results in the past four years has shown, however, that the structure of these network glasses is not all that random. Specifically, Raman[2] and Mössbauer-spectroscopy[3] experiments show that some fraction of like-atom bonds $A-A$ and $B-B$ appears to be an intrinsic feature of the completely relaxed stoichiometric $GeSe_2$ and GeS_2 bulk glasses. The presence of a finite and reproducible broken chemical order and particularly its composition dependence in $A_{1-y}B_{2+y}$ glasses (A denotes Ge and B denotes S or Se) indicates that the microscopic origin of these like-atom bonds cannot be due to isolated bonding defects in a completely polymerized $A(B_{1/2})_4$ network.

To quantitatively understand the observation of broken chemical order, it has been suggested[3,4] that these AB_2 glasses consist of at least two types of morphologically and stoichiometrically distinct large molecular clusters, analogous to donor and acceptor molecules in molecular crystals. In this molecular-cluster-network (MCN) model, proposed by Phillips,[4] cluster surfaces play an integral role in determining the glass-forming tendency. In this model the degree of broken chemical order is derived from the surface to volume ratio or the size of the clusters.

This new conceptual approach has suggested several interesting possibilities for inducing a transformation of a network from its partially polymerized state as in a MCN to a completely polymerized state as in a CRN. One can imagine that erasure of like-atom bonds accompanied by the fusion of cluster interfaces in an AB_2 glass can be affected in one of several ways: (a) optically,[2] (b) thermally, (c) by hydrostatic pressure,[5] and (d) chemically by alloying. Griffiths *et al.*[2] have recently demonstrated feasibility of case (a) outlined above. These workers have observed photoinduced reversible reconstruction of a bulk $GeSe_2$ glass network from its virgin MCN state to a CRN ("quasicrystalline") state with the help of sub-band-gap photons. In this experiment the reconstruction was detected optically using Raman spectroscopy. Recently, Murase and Fukunaga[5] have reported the observation, by optical means, of a pressure-induced reversible structural phase transition in g-$GeSe_2$ at $P=49$ kbar. The high-pressure phase is believed to be a quasi-three-dimensional network (CRN) in which the chemical order of the network is nearly completely restored. For $GeSe_2$, we have succeeded in demonstrating the feasibility of case (d) by both anion and cation pseudobinary alloying using nuclear-resonance spectroscopy. Experiments on anion (Te) alloying involved studying the broken chemical order in pseudobinary $GeSe_{2-x}Te_x$ glasses using both emission[6] and absorption[7] Mössbauer spectroscopy. Brief reports on that work have appeared elsewhere. In the present paper we provide details of experiments involving erasure of like-atom bonds in $GeSe_2$ glass by cation (Sn) alloying.[8] The chemical order in ternary glasses of the type $Ge_{1-x}Sn_xSe_2$ has been probed as a function of x using both ^{119}Sn Mössbauer spectroscopy and Raman spectroscopy. We will show that the MCN of $GeSe_2$ glass transforms to a CRN at $x=X_c=0.35$. This may well represent the first realization[9] of a strongly chemically ordered, fully polymerized melt-quenched glass stable at normal temperature and pressure.

In Secs. II and III of this paper we present details of the experiments undertaken and results obtained. In Sec. IV we identify the Mössbauer sites and Raman vibrational modes. In Sec. V we interpret these in terms of a universal structural phase transition in network glasses. We summarize the principal conclusions emerging from our work in Sec. VI.

II. EXPERIMENTAL CONSIDERATIONS

The experimental procedure consisted of preparing melt-quenched glasses of composition $Ge_{1-x}Sn_xSe_2$ and recording spectra as a function of x. All samples appeared to be homogeneous glasses, as characterized by their glass transitions studied by differential scanning calorimetry. Some of the glasses were subsequently crystallized by heating to T_x. The crystallization behavior of these ternary glasses will be discussed in greater depth in a forthcoming paper.

A. Sample preparation

Small bulk glasses of 0.25 g size were made by alloying the pure elements in vacuum-sealed quartz tubes of 5 mm i.d. at approximately 950 °C. The quartz tubes were held vertical, enabling the melts to uniformly mix and homogenize. 99.9999%-pure elemental Sn and Se from Spex Industries and 99.999%-elemental Ge from Cerac, Inc. were used as starting materials. After homogenizing the melts at 950 °C for 1 or 2 d, the temperature was lowered in increments as large as 250 °C and the melts equilibrated at this lower temperature for an additional 1 or 2 d before water-quenching. Glasses exhibiting reproducible Mössbauer spectra could be made in this manner for the composition range $0 < x < 0.6$.

It was also our experience that if the melt size is increased to 0.40 g, water-quenching invariably leads to partially crystalline samples. This is in accord with the findings of Fukunaga *et al.*,[10] who could not obtain completely glassy samples in the present ternary phase for $x > 0$ in working with 10-g samples. There is evidence that c-SnSe appears to precipitate in the interior of such large bulk samples. Apparently the quench rates accessible by water-quenching are not sufficiently high to render larger melts completely glassy.

B. Scanning calorimetry

A Perkin-Elmer model 1B differential scanning calorimeter at a conventional scan rate of 10 K/min was utilized to study the glass-transition endotherm. The glass-transition temperatures were systematically measured as a function of x, and the results are summarized in Fig. 1.

C. Raman spectroscopy

Raman spectra of the bulk glasses were taken in a backscattering geometry using the 5145-Å exciting line from an Ar-ion laser. The scattered light was collected with a 50-mm high-quality camera lens and analyzed with a Spex double spectrometer. The spectral resolution of the system was approximately 2 cm^{-1}. A laser power of 40 mW was used in all measurements. This was done to prevent high-power densities from locally heating and crystallizing the glass samples. In our geometry, crystallization of the glass samples was first observed to occur when a laser power of 120 mW was used.

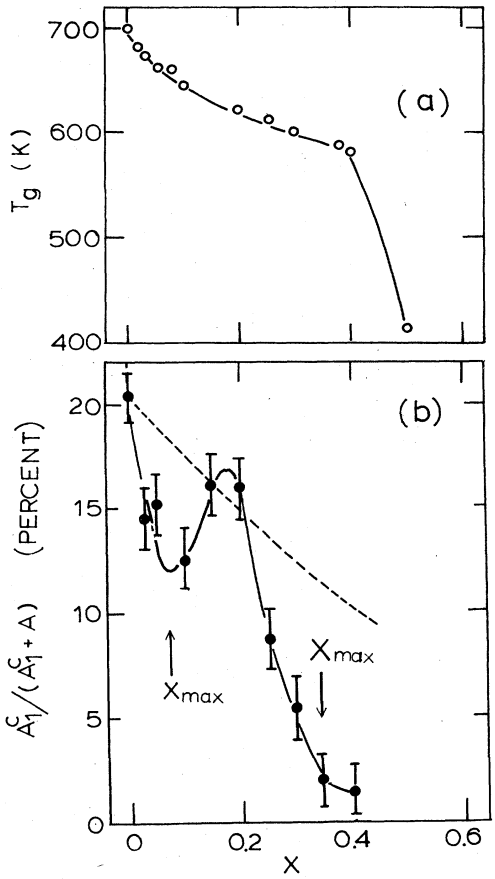

FIG. 1. (a) Glass transitions (T_g) of $Ge_{1-x}Sn_xSe_2$ glasses plotted as a function of x. (b) Normalized $A_1^c/(A_1^c+A)$ scattering strength of the $A_1^c-Ge(Se_{1/2})_4$ companion mode in Raman spectra of $Ge_{1-x}Sn_xSe_2$ glasses plotted as a function of x. Here, A represents the sum of the $A_1-Ge(Se_{1/2})_4$, $A_1-Sn(Se_{1/2})_4$, and $A_1^c-Sn(Se_{1/2})_4$ mode strengths. The dashed line is the expected x variation of the A_1^c-mode strength in a model where Sn randomly replaces Ge in the $GeSe_2$ network. The observed extinction of the A_1^c mode near $x=0.40$ indicates that a structural transition occurs in these glasses between $x=0.20$ and 0.40. The secondary maximum near $x=0.20$ may arise from an intermediate stage in cluster degradation, where the six-chain "rafts" present at $x=0$ are replaced by two-chain "rafts." See Fig. 8 for details.

D. Mössbauer spectroscopy

Mössbauer spectra of the glasses were recorded using a conventional constant-acceleration drive. A 2-mCi source of ^{119}Sn in $CaSnO_3$ was used to populate the 23.8-keV Mössbauer level. Both the source and absorber were cooled in an exchange-gas Dewar system. Spectra were recorded at 78 and 4.2 K. Data reduction was done[11] on an Apple computer using a least-squares analysis. The spectra were plotted on an IBM digital plotter interfaced to the Apple computer.

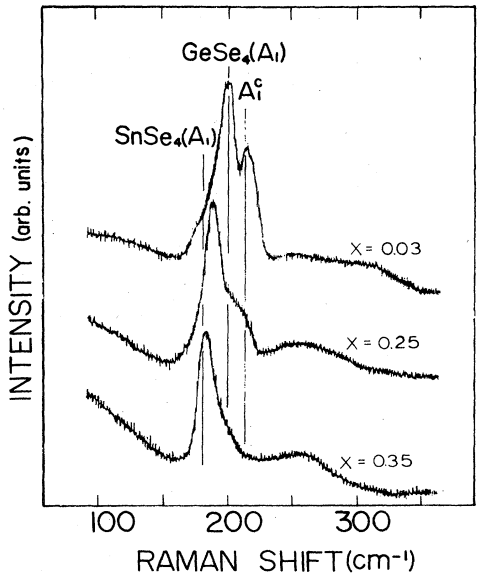

FIG. 2. Raman spectra of $Ge_{1-x}Sn_xSe_2$ glasses at indicated compositions (x). Note the red shift of the A_1-mode frequency with increasing x. This is due to the reduced Sn—Se stretching force constant in tetrahedral $Sn(Se_{1/2})_4$ units formed at the expense of $Ge(Se_{1/2})_4$ units. Also, the A_1^c-mode scattering strength declines to the point where at $x=0.35$ it is barely visible.

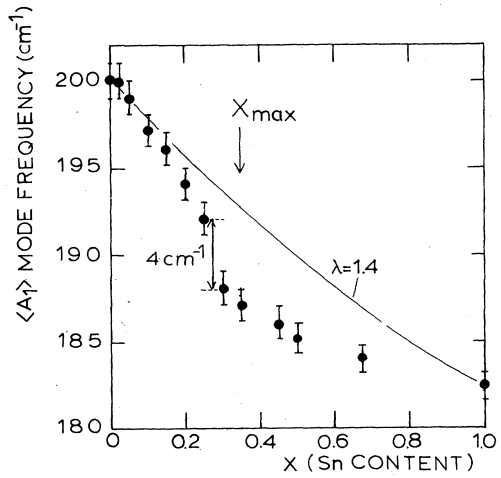

FIG. 3. x dependence of $\langle A_1 \rangle$-mode frequency obtained from the Raman spectra of $Ge_{1-x}Sn_xSe_2$ glasses. The point at $x=1$ is taken from the Raman spectrum of an rf-sputtered $SnSe_2$ film. Note the steplike jump in $\langle A_1 \rangle$ seen near $x=0.27$. The smooth curve represents plots of Eq. (4) for the indicated λ value.

III. EXPERIMENTAL RESULTS

A. Differential scanning calorimetry

Figure 1 provides a summary of the glass transitions T_g measured as a function of Sn content x in the $Ge_{1-x}Sn_xSe_2$ ternary glass. Our T_g value for a sample at $x=0$ is in accord with previous measurements on $GeSe_2$ glass reported by Sarrach *et al.*[12] $T_g(x)$ decreases monotonically as the amount of Sn in the glasses increases, and there appears to be two regions to this curve. One for $x<0.40$, in which the T_g decreases relatively slowly from point to point, and a second, for $0.40<x<0.50$, where T_g drops almost by 200 K in a narrow composition range with what appears to be a steplike behavior.

B. Raman spectroscopy

Figure 2 reproduces Raman spectra of $Ge_{1-x}Sn_xSe_2$ ternary glasses at selected values of x. Our Raman spectra of a ternary glass at $x=0.03$ are very similar to previously published[13] spectra of the $GeSe_2$ glass. In the bond-stretching regime, we observe the A_1 and A_1^c modes at 198 and 213 cm^{-1}, respectively. In the spectrum we also see a low-frequency shoulder to the A_1 mode at 180 cm^{-1}, which also has been reported in the spectrum of $GeSe_2$ by other workers.[13,14] Upon alloying $GeSe_2$ with $SnSe_2$, two noteworthy changes occur: The principal A_1 mode red-shifts in a manner that is displayed in Fig. 3, and, second, the intensity of the A_1^c mode reduces to nearly zero as x approaches $0.35=X_{max}$. In Sec. III C we will formally introduce x_{max} and X_{max} as the special x values where the Mössbauer-site intensity ratio $T(x)$ displays a local maximum (see Fig. 6). In Fig. 1(b), we plot the x dependence of the A_1^c-mode strength suitably normalized. A qualitatively similar result has been reported by Murase *et al.*[15] in $Ge_{1-x}Sn_xS_3$ glasses as $x\rightarrow 0.4$. A more subtle observation in our Raman spectra is as follows. In the spectrum of the ternary glass at $x=0.35$, one can see a qualitative enhancement in scattering strength in the vicinity of 260 cm^{-1}. This feature appears to become more prominent for glasses with $x>0.35$. A microscopic interpretation of the local modes will be provided in Sec. IV in connection with the evolution of the glass network with increasing x.

C. Mössbauer spectroscopy

^{119}Sn Mössbauer spectra of $Ge_{1-x}Sn_xSe_2$ glasses at selected compositions are displayed in Fig. 4. These spectra in general display two types of sites:[3] an intense narrow absorption centered at $v=1.55$ mm/s labeled site A and a weak absorption near $v=3.2$ mm/s which forms part of a quadrupole doublet as site B. The other member of the site-B doublet partially overlaps the site-A resonance and is easily deconvoluted by least-squares analysis. We have analyzed these spectra in terms of two sites. The shift (δ) and quadrupole-splitting (Δ) parameters of the sites, and particularly their x dependence, are displayed in in Fig. 5.

It is abundantly clear from the data of Fig. 5 that the microscopic character of site A remains x independent in the range studied. For site B we find that the Mössbauer parameters change drastically with x in the range $0<x<0.15$ and, furthermore, become x independent in the range $0.15<x<0.35$. For $x>0.35$, a small but distinct discontinuity in the parameters can be inferred from the available systematics. We suggest that this discon-

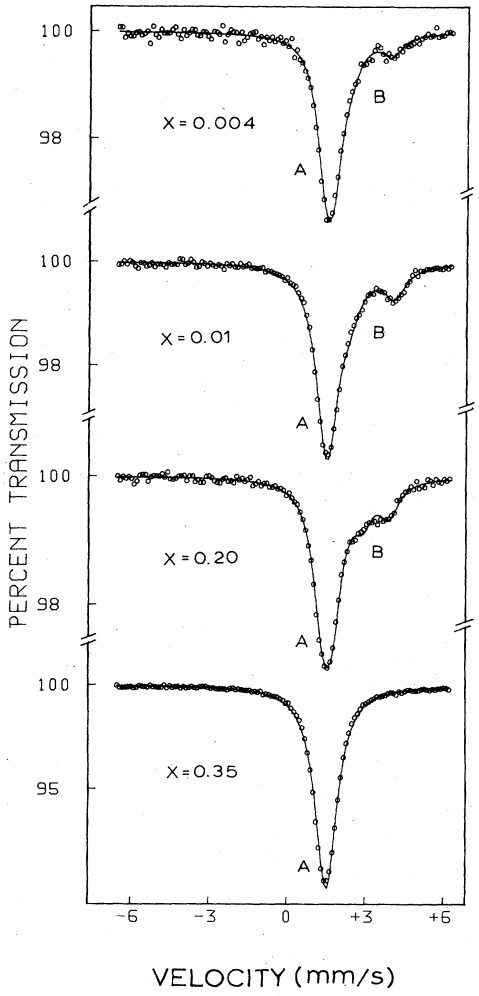

FIG. 4. Mössbauer spectra of $Ge_{1-x}Sn_xSe_2$ glasses for indicated compositions (x) are plotted. Note the absence of a B site in the $x=0.35$ spectrum.

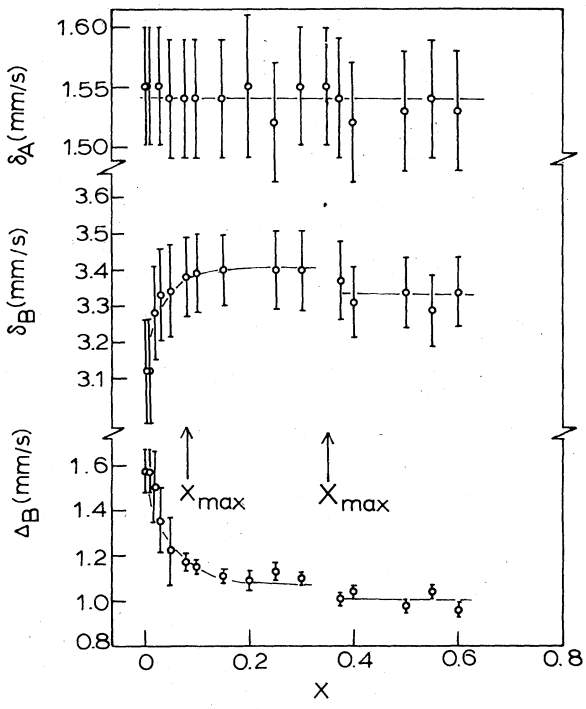

FIG. 5. ^{119}Sn Mössbauer parameter of sites A and B seen in $Ge_{1-x}Sn_xSe_2$ glasses plotted as a function of x. The A-site isomer shift (δ_A) is found to be constant as a function of x. However, the B-site parameters (δ_B and Δ_B) show marked variation with x in the range $0<x<0.15$, and become nearly independent of x for $x\gtrsim 0.15$. Note that there is a discontinuity in these B-site parameters at $x=0.35$.

tinuity represents a change in the microscopic character of B sites when $x>X_{\max}=0.35$. Further discussion of this point will be developed in Sec. V.

From a structural point of view, perhaps some of the most revealing Mössbauer results derive from the x dependence of the site intensities (I_A and I_B). We define the ratio

$$T(x)=\frac{I_A}{(I_A+I_B)} \tag{1}$$

and plot its x dependence in Fig. 6. We note that $T(x)$ exhibits two local maxima: one at $x=x_{\max}=0.07$, where $T=0.88$, and the second at $x=X_{\max}=0.35$, where $T\cong 1$. The latter maximum represents a truly remarkable observation. It implies that a ternary glass of the privileged composition $x=0.35$ possesses only type-A sites. In Sec. V we show that the erasure of B sites concomitant with the extinction of A_1^c-mode strength, as discussed earlier in Sec. III B, at this privileged composition, is the signature of a change in microstructure of the network from a heterogeneous to a homogeneous morphology. For comparison purposes in Fig. 6 we have also shown the $T(x)$ systematics for the corresponding S-containing glasses taken from the work of Grothaus and Boolchand.[16]

IV. DISCUSSION OF RESULTS

We begin our discussion of the results by identifying the microscopic nature of the Mössbauer sites (A and B) populated in the $Ge_{1-x}Sn_xSe_2$ glasses from the nuclear hyperfine structure. Next, we comment on the origin of the local modes seen in the Raman spectra of the glasses. These preliminaries will enable us to discuss model-dependent interpretations of the experimental results in Sec. V.

A. Mössbauer-site identification

1. Site A

On a ^{119}Sn isomer-shift scale (Fig. 7), the shift δ_A lies in a region between Sn^{4+} and Sn^{2+}, which is characteristic of an sp^3 tetrahedrally coordinated covalently bonded Sn site. Specifically, it has been shown by us[17] that the shift δ_A forms part of a trend that is observed in isostructural SnX_4 species (where X denotes O, S, Se, Te, Cl, Br, or F) as a function of the electronegativity difference $\chi_p=\chi_{Sn}-\chi_X$. Quantitatively, we are able to understand

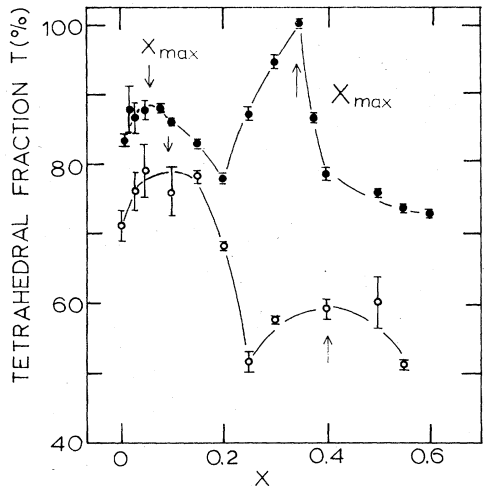

FIG. 6. Mössbauer tetrahedral Sn fraction $T(x) = I_A/(I_A+I_B)$ plotted as a function of x for $Ge_{1-x}Sn_xSe_2$ glasses (●) and $Ge_{1-x}Sn_xS_2$ glasses (○). The two-peak structure of $T(x)$ seen in the selenide glass is discussed in the text. Note that for $x=0.35$, $T=1$.

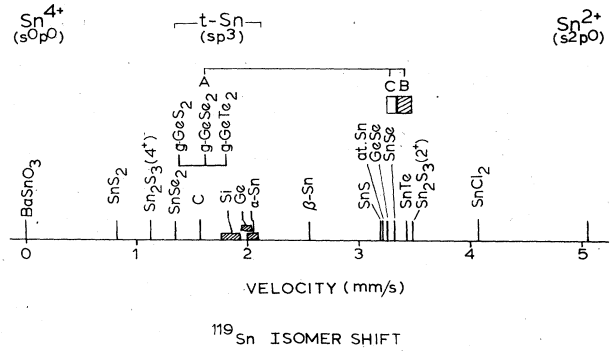

FIG. 7. ^{119}Sn Mössbauer isomer-shift scale showing isomer shifts in selected Sn-bearing crystals and glasses.

the magnitude of these shifts in terms of covalently bonded interactions that are modified by ionic or charge-transfer contributions. The reader is referred to the extensive discussion of this point in Ref. 17. We identify the δ_A shift with Sn replacing a Ge site in a local tetrahedral unit of $Ge(Se_{1/2})_4$. If Sn were octahedrally coordinated to six Se near neighbors, as in the model compound c-$SnSe_2$, one would expect the shift to be $+1.34$ mm/s, i.e., 0.21 mm/s less than the value of $\delta_A = 1.55(5)$ mm/s presently observed. These observations contribute strong microscopic evidence for the fact that site A represents Sn that is present in a local $Sn(Se_{1/2})_4$ tetrahedral unit.

The shift δ_A *per se* is unable to resolve an important related question, viz., whether the tetrahedral $Sn(Se_{1/2})_4$ units are formed isolated in a network of $Ge(Se_{1/2})_4$ units, or, alternatively, they form part of a phase-separated Sn-rich tetrahedral cluster of $SnSe_2$ stoichiometry. We have recently addressed[17] this question by contrasting the crystallization behavior of a Sn-rich ($x > \frac{1}{2}$) glass to a Sn-poor ($x < \frac{1}{2}$) glass in this ternary, and we find radical differences. These differences are discussed in Ref. 17. These observations and others lead us to conclude that the A sites seen in the present Sn-poor ternary glasses represent isolated tetrahedral $Sn(Se_{1/2})_4$ units that are formed in a network of $Ge(Se_{1/2})_4$ units.

The negligible value of the quadrupole splitting Δ_A constitutes strong independent evidence for the tetrahedral character of Sn coordination in a $Sn(Se_{1/2})_4$ local unit. As is well known, the quadrupole splitting Δ_A in open p-shell elements is extremely sensitive to the local symmetry of the Mössbauer probe atom. It measures the local electric field gradient (EFG) at the Sn site through the usual relation

$$\Delta = \tfrac{1}{2} e^2 V_{zz} Q (1+\eta^2/3)^{1/2} . \tag{2}$$

In tetrahedral geometry,

$$eV_{zz} = -\frac{4e}{5\langle r^3\rangle}\left[U_z - \frac{U_x+U_y}{2}\right] \tag{3}$$

vanishes because the p_x-, p_y-, and p_z-orbital populations U_x, U_y, and U_z are identical. The origin of the small but nonzero value of Δ_A inferred from our experiments has several possibilities. First, our experiments show that the value of Δ_A in g-$GeSe_2$ and c-$GeSe_2$ are identical. This could be a Jahn-Teller distortion induced by Sn when it replaces Ge in a $Ge(Se_{1/2})_4$ unit. Alternatively, this slightly broken tetrahedral symmetry could be an intrinsic feature of the host $Ge(Se_{1/2})_4$ tetrahedral units comprising the molecular structure of both g-$GeSe_2$ and c-$GeSe_2$. In the latter instance, the Sn guest atom merely inherits the distortion when it replaces Ge in such a unit. This latter interpretation is supported by calculations of the ^{119}Sn EFG in the high-temperature phase of c-$GeSe_2$ using the extended Hückel procedure.[18] These calculations yield a value of Δ_A in agreement with our observed value, when we assume that Sn merely occupies Ge sites of the network. This is a point which shall be elaborated on in a forthcoming paper.[18]

2. *Site B*

The origin of B sites in a $GeSe_2$ glass was discussed earlier[3] by us in connection with Mössbauer-site intensity populations in Sn-doped Ge_xSe_{1-x} bulk glasses. These sites were identified with Sn replacing Ge in an ethanelike linearly polymerized cluster, $Ge_2(Se_{1/2})_6$. In such a cluster, Sn is locally coordinated to three Se near neighbors and one Ge near neighbor. The lack of tetrahedral chemical symmetry in such a local unit induces a large Δ_B. This is so because Sn in such a cluster is present in a largely $2+$ state, as revealed by the large positive shift,

TABLE I. Comparison of Mössbauer parameters of the B site in $Ge_{1-x}Sn_xSe_2$ glasses for $x > X_{max}$ and of c-SnSe.

Host	δ (mm/s)	Δ (mm/s)
B-site ($x > X_{max}$)	3.33(10)	1.02(4)
c-SnSe	3.31(2)	0.74(2)

δ_B. The largely divalent character of Sn can be reconciled in terms of atomic-size considerations of the guest Sn atom in such a molecular unit, and is a point discussed earlier.[17,18]

The rapid x variation of both δ_B and Δ_B in the range $0<x<X_{\max}$ is in sharp contrast to the lack of variation of the corresponding parameters of site A. We associate this rapid x variation of site-B parameters with the low dimensionality of this cluster, and, in particular, to a systematic relaxation of the intercluster (cluster-B—cluster-A) interaction upon alloying $GeSe_2$ glass with $SnSe_2$. We have investigated the underlying microscopic mechanism by calculating the EFG in characteristic molecular clusters. Results of these calculations will be discussed elsewhere.[18]

For $x>X_{\max}$, the evidence of a mild break in the $\delta_B(x)$ and $\Delta_B(x)$ parameters is due to a microscopic change in the nature of B sites. We are struck by the close similarity of these parameters with those of crystalline SnSe (see Table I). On this basis we argue that the B sites seen for $x>X_{\max}$ represent a segregated Sn-rich amorphous SnSe phase in which Sn^{2+} is present in a distorted octahedral arrangement of Se^{2-} anions. Apparently, in this composition range, Sn largely phase-segregates into this amorphous phase, as evidenced by a monotonic decrease in $T(x)$. This particular interpretation of B sites is further supported by our Raman measurements, which are discussed next.

B. Raman spectroscopy and local A_1 and A_1^c modes

The A_1 mode at 198 cm^{-1} in $GeSe_2$ has been unambiguously identified by a number of previous workers[13] as a symmetric breathing mode of a $Ge(Se_{1/2})_4$ tetrahedral unit, while the A_1^c mode at 213 cm^{-1} is generally taken to be signature of medium-range order of the glass network.[14] The microscopic origin of the A_1^c mode as a cluster-edge mode is supported by recent photostructural transformation studies[2] and vibrational density-of-states calculations.[19]

The effect of alloying $GeSe_2$ with $SnSe_2$ is to systematically red-shift the A_1 mode at 198 cm^{-1}. This is due primarily to the larger Sn mass, as well as a reduced Sn—Se stretching force constant in tetrahedral $Sn(Se_{1/2})_4$ units. It is for this reason, for example, that, in sputtered a-$SnSe_2$, which is shown to be predominantly a tetrahedral network,[20] we find a lower A_1-mode frequency of 182 cm^{-1}. For intermediate compositions, deconvolution of the A_1 mode into an A_1-Ge mode and an A_1-Sn mode is, at best, difficult. This is because the A_1-mode frequencies, as well as their scattering strengths, can be expected to change with x on account of the weak but nonzero intertetrahedral interactions. The presence of these subtle effects is best inferred by plotting the $\langle A_1\rangle$-mode frequency versus x. We define $\langle A_1\rangle$ as the frequency of the observed peak in the Raman spectra. This turns out to be an experimentally well-defined quantity because the total red shift in the A_1-mode frequency, $A_1^{Ge}-A_1^{Sn}=16$ cm^{-1}, is of the order of the linewidth of the A_1 modes. Under such conditions, one can write

$$\langle A_1\rangle \simeq \frac{A_1^{Ge}(1-x)+\lambda x A_1^{Sn}}{1+(\lambda-1)x}\ , \tag{4}$$

where λ is an adjustable parameter. Upon keeping the end values fixed at $A_1^{Ge}=198$ cm^{-1} and $A_1^{Sn}=182$ cm^{-1}, and taking $\lambda=1.4$ in Eq. (4), one finds that this equation does not adequately account for the observed $\langle A_1(x)\rangle$ behavior (Fig. 3). This is significant because the value of λ that we chose, 1.4, actually represents the ratio of the absolute Raman cross section[21] of A_1 modes of isolated $SnCl_4$ to $GeCl_4$ units. This ratio should presumably also provide the A_1 polarization normalization for isolated $Sn(Se_{1/2})_4$ to $Ge(Se_{1/2})_4$ tetrahedral units. We find from Fig. 3 that a substantially larger λ value is needed to describe the data, and, in particular, for $x<X_{\max}$, a value of $\lambda=2.5$, while for $x>X_{\max}$, a value of $\lambda=4.0$ is satisfactory. These striking changes in weight enhancement are the result of changing intertetrahedral couplings of the network glass. For small x values, isolated $Sn(Se_{1/2})_4$ units are formed, embedded in a predominantly $Ge(Se_{1/2})_4$ network which is known to be in a state of high stress as revealed by pressure-dependent Raman studies of Murase *et al.*[15] Upon increasing x, the network, in general, relaxes, since tetrahedral Sn sites act as stress-releasing centers. The intertetrahedral couplings of $Sn(Se_{1/2})_4$ units are presumably weaker than of $Ge(Se_{1/2})_4$ units. When $x\rightarrow X_{\max}$, a major reorganization of the network occurs in which both $Sn(Se_{1/2})_4$ and $Ge(Se_{1/2})_4$ units become markedly decoupled. The sharp steplike lowering of $\langle A_1(x)\rangle$ by 4 cm^{-1} that occurs over a narrow composition range $0.25<x<0.30$ is reminiscent of a qualitatively similar effect seen by Magana and Lannin[22] in Raman spectra of glassy and liquid $GeSe_2$. In liquid $GeSe_2$, the A_1 mode red-shifts by about 6 cm^{-1} in relation to glassy $GeSe_2$. These observations suggest that the steplike behavior seen in our ternary glass (Fig. 3) is driven primarily from a red shift of the A_1^{Ge} modes as the network stress first begins to be released near $x=0.25$. Obviously, this stress-release mechanism (unclamping effect) is more pronounced in the glass-to-liquid transition than in the glass-to-glass transition. This cooperative unclamping leads to a morphological phase transformation in the present ternary glass at $x=0.35$. We will return to this point in Sec. V.

In concluding this section, we would like to make a final observation. Our Raman spectra of Fig. 2 also provide qualitative evidence for an enhancement of scattering strength near 260 cm^{-1} when $x>X_{\max}$. This enhancement in scattering could arise from a narrowing of the $Ge(Se_{1/2})_4$ F_2-band upon chemical ordering of the glass. For $x>X_{\max}$, continued growth of scattering at 260 cm^{-1} most probably results from, among other modes, Se_n chainlike Se—Se stretching modes. In the present ternary glass, apparently some degree of phase separation of the glass network occurs into a Se-rich cluster and Se-poor clusters when $x>X_{\max}$. The Se-rich cluster presumably consists of Se_n chains or ringlike fragments, as found in amorphous Se, while the Se-deficient cluster consists of an amorphous distorted octahedral SnSe phase. The latter phase provides the B signal in the Mössbauer experiments. The stoichiometric relation governing this phase separation is then

$$n\ SnSe_2 = n(a\text{-}SnSe) + Se_n\ , \tag{5}$$

with the remainder of the glass network consisting of tetrahedral units. The growth in the Mössbauer B-site intensities for $x > X_{max}$ (Fig. 6) concomitant with an increase in Raman scattering strength of the 260-cm^{-1} mode provide justification for this phase separation.

V. MODEL INTERPRETATION OF SPECTROSCOPIC DATA

In preceding sections we have identified the local modes seen in Raman spectra, and the different types of Sn sites observed in the Mössbauer spectra of the present $Ge_{1-x}Sn_xSe_2$ ternary glass. These identifications already limit the scope of structural models that can be used to describe the present glasses, but perhaps the most severe restrictions on modeling these network glasses arise from the x variation of the Mössbauer-site intensity ratio $T(x)$ and the A_1^c Raman strength. We will conclude this section by showing that our spectroscopic data provide strong evidence of a structural phase transition involving a change in microphase morphology of the present ternary glass with composition.

Our definition of $T(x) = I_A/(I_A + I_B)$ and the identification of A sites as tetrahedral Sn sites lends a precise meaning to $T(x)$. It represents the fraction of Sn sites that are present in both a chemically and geometrically tetrahedral environment in the network. This statement is subject to the following minor qualification. In Mössbauer spectroscopy, generally speaking, site intensities (I) are related to site populations (N) through the site recoil-free fraction (f):

$$I_X = f_X N_X \quad \text{where } X = A,B\ . \tag{6}$$

Consequently,

$$T(x) = \frac{f_A N_A}{f_A N_A + f_B N_B} = \frac{N_A}{N_A + (f_B/f_A)N_B}\ , \tag{7}$$

where $f_{A(B)}$ and $N_{A(B)}$ represent the site recoil-free fractions and populations, respectively. Consequently, the simple relation

$$T(x) = \frac{N_A}{(N_A + N_B)} \tag{8}$$

is valid only if $f_A = f_B$. Temperature-dependent measurements of the Mössbauer f factor in g-$GeSe_2$ have been performed in our laboratory and these show that, at $T = 4.2$ K, $f_B/f_A = 0.94$. In other words, corrections to $T(x)$ on account of the f factors amount to about 5%, and this is comparable to the error in measurement of $T(x)$ itself. Furthermore, this correction term to first order, is expected to be independent of x and, henceforth, will not be considered in our quantitative discussion of the trends of $T(x)$ which show the two-peak structure (Fig. 6).

A. Structural interpretation of spectroscopic results on $Ge_{1-x}Sn_xSe_2$

1. Composition $x \cong 0$

To analyze the structural implications emerging from the present spectroscopic results, we will now study the x variation of A_1^c-mode strength [Fig. 1(a)], the $\langle A_1(x)\rangle$-mode frequency (Fig. 3), and $T(x)$ (Fig. 6). The starting point for this discussion is the end-member composition ($x = 0$). $T(x=0) = 0.84$ implies the existence of an 0.16 fraction of nontetrahedral Ge sites in $GeSe_2$ bulk glass. We have previously shown[3] that the microscopic origin of this broken symmetry can be quantitatively understood in terms of a MCN consisting of a specific Se-rich cluster of $Ge_{22}Se_{46}$ stoichiometry and a Ge-rich cluster of Ge_2Se_3 stoichiometry. The stoichiometric relation governing this molecular phase separation is approximately given by

$$26\ GeSe_2 = Ge_{22}Se_{46} + 2\ Ge_2Se_3\ . \tag{9}$$

The Se-rich cluster (shown in Fig. 8) consists of a fragment of the high-temperature phase of c-$GeSe_2$, which has been terminated laterally (along the b axis) by Se—Se bonds. This cluster differs from the original "outrigger raft" proposal of Phillips[4] in that it has nearly 3 times the lateral width. There are six corner-sharing chains running along the b axis instead of two. The length of the "rafts" along the a axis is unknown. All Ge sites present in this cluster, in principle, are possible A sites, while one of the two Ge sites in the ethanelike clusters could be the B sites seen in Mössbauer spectroscopy. Because Sn randomly selects[3] A- and B-type Ge sites, the observed Sn tetrahedral fraction equals the Ge tetrahedral fraction of the glass network.

According to Eq. (9), since there are four B-type Ge sites for every 22 A-type Ge sites, the fraction $1-T$ of chemically nontetrahedral sites (degree of broken chemical order) is

$$1 - T = \frac{N_B}{(N_A + N_B)} = 4/26 = 0.154\ , \tag{10}$$

and this is in accord with our experimental result, 0.16. In Raman spectroscopy, where scattering strengths scale as the number of bonds, it is immediately apparent from Eq. (9) that the same degree of phase separation will lead to two homopolar (Ge—Ge) bonds for every 100 heteropolar (Ge—Se) ones. If the scattering strengths of the Ge—Se bond and Ge—Ge bond are taken to be the same (which may seem unlikely *a priori*), it becomes transparent, from Fig. 2, that the observed scattering strength ratio of the 180-cm^{-1} mode (A_{1g} ethanelike mode) to the 202-cm^{-1} mode (A_1 mode) of 3% or so (see Nemanich *et al.* in Ref. 1) is in surprisingly good agreement with the present model of molecular phase separation for $GeSe_2$ glass, which gives the fraction of Ge—Ge bonds, $f_G = N(\text{Ge—Ge})/N(\text{Ge—Se}) = 0.02$. It is of interest to compare our measured estimate of the fraction of Ge—Ge bonds, $f_G = 0.02$, with the value that can be obtained by assuming that bond energies are mutually independent (i.e., no bond-bond interactions). We also assume that f_G is independent of topological or packing constraints. Then,

$$f_G = \exp(\Delta H_f/2kT_g)\ , \tag{11}$$

where ΔH_f is the heat of formation per $GeSe_2$ formula unit, each of which contains four shared (two unshared) Ge—Se bonds. With $T_g = 700$ K and $\Delta H_f = -21.7$ kcal/mol,[23] Eq. (11) gives $f_G = 0.0002$, i.e., 2 orders of

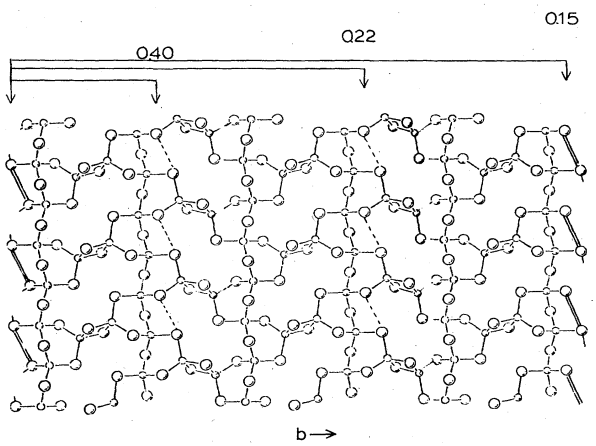

FIG. 8. Fragment of the high-temperature phase of c-$GeSe_2$ showing corner-sharing chains running laterally along the b axis. The small circles represent fourfold coordinated Ge atoms, while the larger circles represent twofold-coordinated Se atoms. In the glass this fragment is believed to be bordered by Se-Se dimers. This fragment, also known as a "raft," is thus Se-rich. The degree of broken chemical order (DBO) of the glass network is "raft"-size dependent. In particular, for a two-chain "raft" the DBO is 0.4, while for a six-chain "raft" the DBO is 0.15. The observed DBO in $GeSe_2$ glass is compatible with a six-chain "raft," i.e., a cluster about 50 Å wide.

magnitude smaller than the measured value. One possible interpretation is that, in g-$GeSe_2$, the population of like-atom bonds is strongly influenced by packing constraints, and the approximation of no bond-bond interactions is invalid. This is independently suggested by molar-volume measurements[24] in the Ge_xSe_{1-x} binary that display a striking maximum at $x=\frac{1}{3}$, i.e, a low-density or open network with a large internal surface area associated with broken chemical order.

2. *Composition range $0<x<0.2$*

We are struck by the x variation of A_1^c-mode strength [Fig. 1(b)], which displays an inverse correlation with $T(x)$, as shown in Fig. 6. Specifically, we note that a local maximum in A_1^c-mode strength corresponds to a local minimum in $T(x)$. In particular, when the A_1^c-mode strength approaches 0 at $x=0.35$, $T=1$. These results are significant for several reasons. First, they demonstrate that both these microscopic observables, which are chemically specific to Sn and Ge, respectively, are direct manifestations of the network structure. Second, this correlation supports the view that the A_1^c mode, like the T fraction, is a signature of incomplete chemical ordering of the glass network. Consequently, we must argue that our results are inconsistent with the identification of the A_1^c mode as merely evidence for medium-range order (of a large ring species embedded) in a chemically ordered network, as suggested by Nemanich *et al.*[1] On the other hand, our results do support the notion that the A_1^c mode is a signature of (a cluster-edge-mode) broken chemical order of the glass network, as first pointed out by Bridenbaugh *et al.*[14]

The two maxima in $T(x)$ can be understood in terms of a MCN description of the alloy glasses as follows. The rapid growth in $T(x)$ in the range $0<x<0.07$ can be qualitatively understood in terms of edge segregation of Sn atoms selectively occupying Ge sites on the two outermost chains (or "logs") of the six-chain-containing $Ge_{22}Se_{46}$ "raft" (Fig. 8). The attendant stress that has accumulated on the surface of this cluster, where reconstructed Se—Se bonds occur, can now be relieved by substituting an atom of larger covalent radius than Ge. Apparently this process rapidly saturates even when only half of the available Ge edge sites in the "raft" structure are occupied. Increasing x above 0.07, we conjecture that this causes the six-chain "raft" to break up into "rafts" of smaller lateral extensions such as a five-chain or even a four-chain "raft." In this composition range, $0.07<x<0.20$, the role of Sn changes. It progressively depolymerizes the layered network prevailing at $x=0.07$. This is clearly evidenced by the increase in the A_1^c-mode strength and the decrease of $T(x)$, both signatures of a higher degree of clustering or broken chemical order. The trend of a growth in population of B sites at the expense of A sites is remarkable because it is just the reverse of what one would have predicted based on ionic or charge-transfer contributions to the nearest-neighbor covalent-bonding energies. Our spectroscopic data highlight the delicate interplay between strain fields and valence force fields that determines the mechanical equilibrium of a network glass.

Further justification for the correctness of these ideas is derived from our results on $Ge_{1-x}Sn_xS_2$ alloy glasses, which are also shown in Fig. 3. These exhibit a similar two-peak structure for $T(x)$ in which $x_{max}=0.10$, i.e., the first peak is shifted towards higher x in relation to the selenide glasses. This trend of a shift in x_{max} to higher x is precisely what one expects to find if a higher degree of broken chemical order prevails in the S-rich cluster in relation to the Se-rich cluster.[9] Chemically, this reflects the greater stability of S—S bonds.[23]

3. *Composition range $0.20<x<0.35$ and universal structural phase transition*

The most profound result to emerge from our experiments is that $T=0.99\pm0.01$ at $x=X_{max}=0.35$ in $Ge_{1-x}Sn_xSe_2$ glasses. The spectacularly complete restoration of chemical order accompanied by the coincident extinction of the A_1^c mode as $x=0.35$ [Fig. 1(b)] constitutes strong evidence of a change in the microphase morphology of the network. We interpret this as a transition of the glass network from a MCN to a CRN. Specifically, the increase of $T(x)$ in the composition range $0.20<x<X_{max}=0.35$ is visualized as a process in which pure and mixed polymerized ethanelike clusters, $Ge_2(Se_{1/2})_6$ and $SnGe(Se_{1/2})_6$, react with the surface of the Se-rich "raft" clusters to restore the broken chemical order. This reformation process involves the breakdown of bonds between nearly homopolar pairs such as Sn—Sn, Sn—Ge, and Se—Se to form the stronger heterpolar Ge—Se and Sn—Se bonds. The extinction of the A_1^c mode is a natural consequence of this bond-reformation process. This then leads to the first realization of a Phillips CRN glass,[9] consisting only of tetrahedral units of $Sn(Se_{1/2})_4$

and $Ge(Se_{1/2})_4$ in the approximate ratio of 1:2. In contrast, the partial restoration of chemical order ($T=0.60$ at $x=X_{max}=0.40$) in $Ge_{1-x}Sn_xS_2$ glasses indicates that the MCN→CRN transition is incomplete, and that some degree of molecular clustering prevails both above and below this transition.[16]

The steplike jump in $\langle A_1(x)\rangle$-mode frequency that occurs near $x=0.27$ (Fig. 3) provides additional insights in the nature of the CRN. Statistical considerations suggest that the compositional width of this steplike jump should decrease with increasing physical size of the clusters involved. Specifically, the sharpness of the jump in $\langle A_1(x)\rangle$ as a function of (x) (Fig. 3) shows that it involves clusters of large microscopic dimensions. This is seen by comparing the present transition width ($\Delta x\sim 0.05$) in the $\langle A_1(x)\rangle$-mode frequency to the transition width ($\Delta x\sim 0.20$) of free (AgBr) to self-trapped (AgCl) exciton that is seen in mixed $AgBr_{1-x}Cl_x$ crystals[25] as x approaches 0.45. Bearing in mind that the size of the hydrogenlike free exciton in AgBr is 10 Å or more, we estimate that the size of molecular clusters involved in the structural phase transition in the present ternary glass is 40 Å or more.

4. *Composition range $0.35<x<0.60$*

In this composition range we visualize the glasses to be phase-separated into three distinct microphase morphologies which consist of the three-dimensional tetrahedral $A(Se_{1/2})_4$ CRN (A denotes Sn and Ge), prevailing at $x=0.35$, a Se-rich Se_n chain or ringlike microphase, and a Sn-rich distorted octahedral amorphous SnSe phase. The reduction in T when $x>0.35$ can be traced to the tendency of Sn to phase-separate into the amorphous SnSe phase. As discussed earlier, in Sec. IV, the B sites seen in this composition range are to be identified with this SnSe phase. The cessation of bulk glass formation when $x>0.60$ can be traced to the tendency of Sn to become sixfold coordinated. The progressive coarsening of the SnSe amorphous phase when $x>0.60$ leads such quenched melts to phase-separate on a macroscopic scale into a predominant Ge-rich amorphous phase and the Sn-rich c-SnSe phase. Recently, we succeeded in preparing a completely amorphous $SnSe_2$ film by rf-diode-sputtering, which shows that phase separation can be partially suppressed by vapor deposition. Raman and Mössbauer-spectroscopic results on $SnSe_2$ indicate that it is a predominantly tetrahedral network with about 10—15% of the Sn atoms present in the amorphous SnSe phase.

B. Continuous—random-network models

Despite the immense popularity[1] of modeling stoichiometric glasses after CRN's, the present results on $Ge_{1-x}Sn_xSe_2$ ternary glass demonstrate that such a structure is the exception and not the rule. As discussed earlier in this section, it is only in a narrow composition range centered around $x=0.35$, where $T\simeq 1$, that one can indeed realize a completely polymerized network of tetrahedral units.

Although oxide glasses such as SiO_2, GeO_2, and B_2O_3 and chalcogenides glasses such as As_2Se_3 and $GeSe_2$ have been modeled after CRN's, this view has been disputed by a more recent reinterpretation of the existing vibrational data.[26] The difference in the degree of polymerization between CRN's and MCN's, at least for $GeSe_2$ and GeS_2, is too subtle to be discriminated by diffraction experiments and/or vibrational spectroscopy alone, particularly when the $8-N$ coordination rule is held intact in both model descriptions.

According to a CRN-model description, one would scarcely expect $T(x)$ to exhibit the two-peak structure (Fig. 6) in the present ternary glass. In fact, one would ideally expect $T(x)$ to be structureless and to have a value of unity. Only if the symmetry-breaking B sites can be identified with isolated point defects in an ordered-bond network can the possibility of invoking a CRN model for the present ternary glass be seriously entertained. At such point defects isolated Sn atoms could condense, increasing the concentration of such defects and reducing $T(x)$ monotonically with increasing x. Such a point-defect model is inconsistent with the oscillations in $T(x)$ that we observe, and, specifically, cannot explain the dramatic peak $T=0.98\pm 0.01$ at $x=0.35$ in $Ge_{1-x}Sn_xSe_2$ alloys. Failures of the CRN model to explain qualitative features of the Raman spectrum of $GeSe_2$ glass have been discussed in detail by Griffiths *et al.*[27]

The nuclear-hyperfine-interaction parameters of B sites rule out two other possible microscopic configurations for these sites. It is difficult, on this basis, for example, to assign B sites to a Sn-rich crystalline impurity phase such as c-SnO or c-SnSe in the ternary glasses. Furthermore, the large change in the isomer shift between A (1.55 mm/s) and B sites (3.31 mm/s) also rules out an additional possibility: B sites result from a geometrically but not chemically distorted tetrahedral environment, while A sites result from a regular tetrahedral one. Differences between edge-sharing and corner-sharing tetrahedral units can, in principle, be expected to change the magnitude of the Δ_B parameter by 10—20%, but such distortions alone could not change the δ_B parameter significantly. The δ_B parameter which probes the contact charge density is due primarily to the population of $5s$-like electrons at the ^{119}Sn nucleus. To first order, this contact charge density is not expected to change if the tetrahedral $Sn(Se_{1/2})_4$ unit is merely distorted.

The arguments for the existence of a CRN at $x=0.35$, on the other hand, are overwhelming. All the objections raised above in the context of B sites clearly do not apply, since in the Mössbauer spectrum no B sites are observed at this composition. This clearly shows that all Sn atoms present in the network occur tetrahedrally coordinated to four Se atoms. Furthermore, since Sn atoms are known to replace tetrahedral and nontetrahedral Ge sites with equal probability,[3] if the latter sites were present in the network one would clearly expect to observe nontetrahedral Sn sites as well. This being not the case, one must conclude that $T\simeq 1$ is also evidence that all Ge cation sites occur tetrahedrally coordinated at $x=0.35$.

The justification for the existence of this morphological transition has been discussed by Phillips[9] on theoretical grounds. One may understand why alloying $GeSe_2$ with

$SnSe_2$ induces a structural phase transformation in terms of topological principles using the idea of force-field constraints. It is well known that although Si and Ge prefer to be fourfold coordinated, the energy difference between fourfold and sixfold coordination for the case of the heavier cation Sn is small at temperatures above room temperature where the white (metallic) Sn phase is stable. This indicates that bond-bending forces for Sn are weak. One can visualize alloying of $GeSe_2$ with $SnSe_2$ as a process that lowers the average number of constraints per atom in the overconstrained $GeSe_2$-glass network. At $x=\frac{2}{5}$ the constraint theory shows that the number of constraints per atom in the present ternary glass equals three, the dimension of the space in which the network is embedded. The process of cation-tuning of force-field constraints by alloying thus provides a good quantitative basis for understanding the structural phase transformation observed by us at $x=X_c$.

VI. CONCLUDING REMARKS

In the $Ge_{1-x}Sn_x(S \text{ or } Se)_2$ cation ternary glasses, we have selected a system with strong chemical order and a very stable building block [the $Ge(Se_{1/2})_4$ tetrahedron] and have tuned the number of constraints by replacing Ge with Sn, i.e., erasing some of the bond-bending constraints associated with fourfold-coordinated sites. In earlier work[6,7] on anion ternary glasses such as $Ge(Te_xSe_{1-x})_2$, more severe network deformation was occurring because the coordination number of Te does not always satisfy the $8-N$ rule. However, behavior similar to that reported here was observed as $x\rightarrow 1$, i.e., the nuclear-quadrupole-resonance parameters tended to a common value. Unfortunately, this value cannot actually be attained in a bulk glass because, for $x>0.6$, devitrification occurs through the disproportionation reaction $GeTe_2=GeTe+Te$. Nevertheless, we believe that other examples of continuous glassy networks can exist. There is some evidence that g-As_2Te_3 is such a system.[28]

In conclusion, we have presented new spectroscopic evidence that points to the existence of a universal transition from a heterogeneous to a homogeneous network morphology for the case of the easy-glass-forming chalcogenides. These and other recent experiments highlight the central role of internal surfaces in stabilizing the glass network against crystallization that has been extensively discussed using a topological theory.[4,9] It is the existence of this transition that most likely is responsible for the profound photostructural effects native to this class of distorted materials.

ACKNOWLEDGMENTS

We are particularly grateful to Dr. J. C. Phillips, Dr. John deNeufville, and Dr. M. Tenhover for many helpful discussions during the course of this work, and to George Lemon, who developed software used in data analysis and plotting Mössbauer spectra. The work at the University of Cincinnati was supported by the National Science Foundation under Grant No. DMR-82-17514.

[1]M. F. Thorpe, in *Vibration Spectroscopy of Molecular Solids,* edited by S. Bratos and R. M. Pick (Plenum, New York, 1979), p. 341. W. H. Zachariasen, J. Am. Chem. Soc. **54**, 3841 (1932); R. J. Nemanich and S. A. Solin, Solid State Commun. **21**, 273 (1977); R. J. Nemanich, G. A. N. Connell, T. M. Hayes, and R. A. Street, Phys. Rev. B **18**, 6900 (1980).

[2]J. E. Griffiths, G. P. Espinosa, J. P. Remeika, and J. C. Phillips, Solid State Commun. **40**, 1077 (1981); Phys. Rev. B **25**, 1272 (1982).

[3]P. Boolchand, J.Grothaus, W. J. Bresser, and P. Suranyi, Phys. Rev. B **25**, 2975 (1982); P. Boolchand, J. Grothaus, and J. C. Phillips, Solid State Commun. **45**, 183 (1983).

[4]J. C. Phillips, J. Non-Cryst. Solids **34**, 153 (1979); **43**, 37 (1981).

[5]K. Murase and T. Fukunaga, in *Proceedings of the Conference on Optical Effects in Amorphous Semiconductors, Snowbird, Utah, August, 1984,* edited by P. C. Taylor and S. G. Bishop (AIP, New York, 1984), p. 449.

[6]W. J. Bresser, P. Boolchand, P. Suranyi, and J. P. deNeufville, Phys. Rev. Lett. **46**, 1689 (1981).

[7]P. Boolchand, W. J. Bresser, P. Suranyi, and J. P. deNeufville, Nucl. Instrum. Methods **199**, 295 (1982).

[8]M. Stevens, J. Grothaus, P. Boolchand, and J. G. Hernandez, Solid State Commun. **47**, 199 (1983).

[9]J. C. Phillips, Solid State Commun. **47**, 203 (1983).

[10]T. Fukunaga, Y. Tanaka, and K. Murase, Solid State Commum. **42**, 513 (1982).

[11]K. J. Sisson and P. Boolchand, Nucl. Instrum. Methods **198**, 317 (1982).

[12]D. J. Sarrach, J. P. deNeufville, and W. L. Hayworth, J. Non-Cryst. Solids **22**, 245 (1976).

[13]P. Tronc, M. Bensoussan, A. Brenac, and C. Sebenne, Phys. Rev. B **8**, 5947 (1973); G. Lucovsky, F. L. Galeener, R. C. Keezer, R. H. Geils, and H. A. Six, *ibid.* **10**, 5134 (1974); G. Lucovsky, R. J. Nemanich, and F. L. Galeener, in *Proceedings of the 7th International Conference on Amorphous and Liquid Semiconductors, Edinburgh, Scotland, 1977,* edited by W. E. Spear and G. C. Stevenson (University of Edinburgh, Scotland, 1977), p. 125.

[14]P. M. Bridenbaugh, G. P. Espinosa, J. E. Griffiths, J. C. Phillips, and J. P. Remeika, Phys. Rev. B **20**, 4140 (1979), and references therein; K. Murase, T. Fukunaga, K. Yakushiji, T. Yoshimi, and I. Yunoki, *Proceedings of the Tenth International Conference on Amorphous and Liquid Semiconductors, Tokyo Japan, August, 1983,* edited by K. Tanaha and T. Shimiza [J. Non-Cryst. Solids **59-60**, 855 (1983).

[15]K. Murase, T. Fukunaga, Y. Tanaka, K. Yakushiji, and I. Yunoki, Physica (Utrecht) **117&118B**, 962 (1983).

[16]J. Grothaus, and P. Boolchand (unpublished).

[17]P. Boolchand and M. J. Stevens, Phys. Rev. B **29**, 1 (1984).

[18]J. Bicerano and P. Boolchand (unpublished).

[19]J. A. Aronovitz, J. R. Banavar, M. A. Marcus, and J. C. Phillips, Phys. Rev. B **28**, 4454 (1983); T. Fukunaga, Ph.D thesis, Osaka University, 1982; K. Murase *et al.*, J. Non-Cryst. Solids **59-60**, 883 (1983).

[20]J. G. Hernandez, J. P. deNeufville, M. J. Stevens, and P. Boolchand (unpublished).

[21]R. Clark and P. D. Mithell, J. Chem. Soc. Faraday Trans. II **71**, 515 (1975); H. Schrotter and H. Klockeur, in *Raman*

Spectroscopy of Gases and Liquids, Vol. 11 of *Topics in Current Physics,* edited by A. Weber (Springer, Berlin, 1979), p. 151. The differential scattering cross section in units of 10^{-48} cm^6/sr is 134 and 96 for the A_1 modes of $SnCl_4$ and $GeCl_4$, respectively.

[22]J. R. Magana and J. S. Lannin, J. Non-Cryst. Solids **59-60**, 1055 (1983).

[23]E. A. Irene and H. Wiedemeyer, Z. Anorg. Allg. Chem. **424**, 277 (1976); J. C. Phillips, Phys. Rev. B **28**, 7038 (1983).

[24]A. Feltz, H. Aust, and A. Blayer, J. Non-Cryst. Solids **55**, 179 (1983).

[25]H. Kanzaki, S. Sakuragi, and K. Sakamoto, Solid State Commun. **9**, 999 (1971).

[26]J. C. Phillips, in *Solid State Physics,* edited by F. Seitz and D. Turnbull (Academic, New York, 1982), Vol. 37, p. 93.

[27]J. E. Griffiths, J. C. Phillips, G. P. Espinosa, J. P. Remeika, and P. M. Bridenbaugh, Phys. Status Solidi B **122**, K11 (1984).

[28]P. Boolchand, W. J. Bresser, and M. Tenhover, Phys. Rev. B **25**, 2971 (1982).